Available online at www.sciencedirect.com
ScienceDirect
Bioorganic & Medicinal Chemistry Letters 17 (2007) 2005–2012
Bioorganic & Medicinal Chemistry Letters

Pyrrolidine-constrained phenethylamines: The design of potent, selective, and pharmacologically efficacious dipeptidyl peptidase IV (DPP4) inhibitors from a lead-like screening hit

Bradley J. Backes,[a,*] Kenton Longenecker,[b] Gregory L. Hamilton,[a] Kent Stewart,[b] Chunqiu Lai,[a] Hana Kopecka,[a] Thomas W. von Geldern,[a] David J. Madar,[a] Zhonghua Pei,[a] Thomas H. Lubben,[a] Bradley A. Zinker,[a] Zhenping Tian,[c] Stephen J. Ballaron,[a] Michael A. Stashko,[a] Amanda K. Mika,[a] David W. A. Beno,[d] Anita J. Kempf-Grote,[d] Candace Black-Schaefer,[b] Hing L. Sham[a] and James M. Trevillyan[a]

[a]*Metabolic Disease Research, Abbott Laboratories, Abbott Park Road, Abbott Park, IL 60064-6099, USA*
[b]*Advanced Technology, Abbott Laboratories, Abbott Park Road, Abbott Park, IL 60064-6099, USA*
[c]*Process Research and Development, Abbott Laboratories, Abbott Park Road, Abbott Park, IL 60064-6099, USA*
[d]*Departments of Exploratory Pharmacokinetics and Pharmaceutics, Global Pharmaceutical Research and Development, Abbott Laboratories, Abbott Park Road, Abbott Park, IL 60064-6099, USA*

Received 13 November 2006; revised 18 December 2006; accepted 8 January 2007
Available online 19 January 2007

Abstract—A novel series of pyrrolidine-constrained phenethylamines were developed as dipeptidyl peptidase IV (DPP4) inhibitors for the treatment of type 2 diabetes. The cyclohexene ring of lead-like screening hit **5** was replaced with a pyrrolidine to enable parallel chemistry, and protein co-crystal structural data guided the optimization of N-substituents. Employing this strategy, a >400× improvement in potency over the initial hit was realized in rapid fashion. Optimized compounds are potent and selective inhibitors with excellent pharmacokinetic profiles. Compound **30** was efficacious in vivo, lowering blood glucose in ZDF rats that were allowed to feed freely on a mixed meal.

Glucagon-like peptide-1 (GLP-1) therapy has emerged as a promising treatment for type 2 diabetes.[1] GLP-1, as an incretin hormone, stimulates insulin biosynthesis and secretion in a glucose-dependent manner while suppressing glucagon release.[2] Thus, blood glucose levels may be regulated by GLP-1 with little risk of hypoglycemia. Additional benefits to patients include the slowing of gastric emptying[3] and a reduction in appetite.[4] Significantly, recent studies in rat suggest that GLP-1 treatment may have the potential to stabilize or even reverse disease progression by increasing β-cell mass and function.[5] Serine protease dipeptidyl peptidase IV (DPP4) inactivates GLP-1(7–36) to give GLP-1(9–36) by cleaving two N-terminal amino acid residues that are required for receptor binding.[6] Accordingly, inhibitors of DPP4 may increase the half-life of active GLP-1, prolonging its beneficial effects. Several clinical trials indicate that orally administered small molecule inhibitors of DPP4 are well-tolerated, lower blood glucose and/or HbA_{1c} levels, and increase glucose tolerance.[7]

Chart 1 lists three notable DPP4 inhibitors that have entered the clinic, vildagliptin **1** (LAF-237),[8] sitagliptin **2** (MK-0431)[9] and saxagliptin **3** (BMS-477118).[10] Our program has produced clinical compound **4** that features an alkyne-substituted cyanopyrrolidine and imparts the inhibitor with a superior selectivity profile.[11] Lead-like[12] cyclohexenyl hit **5** was identified in a high throughput screen of our corporate compound collection as a relatively weak inhibitor of DPP4

Keywords: DPPIV inhibitors; Diabetes; Structure-based design.
* Corresponding author. Tel.: +1 847 938 3521; fax: +1 847 938 1674; e-mail: bradley.backes@abbott.com

0960-894X/$ - see front matter © 2007 Elsevier Ltd. All rights reserved.
doi:10.1016/j.bmcl.2007.01.026

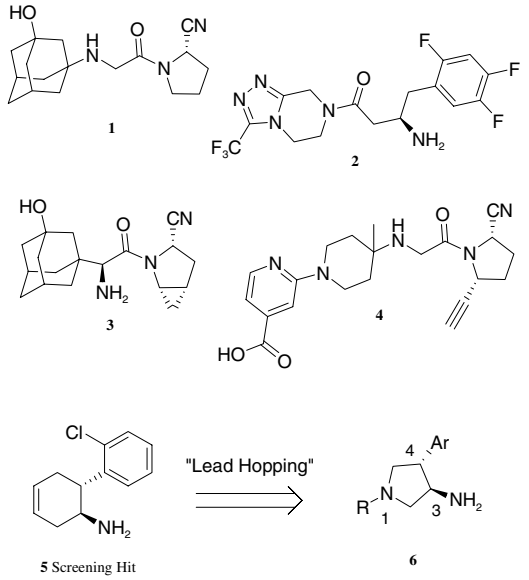

Chart 1. DPP4 inhibitors.

($K_i = 0.8\,\mu M$). However, the high binding efficiency[13] and novel structure of **5** were compelling.[14] We proposed that 'lead-hopping' to **6** would: (1) display the key phenethylamine pharmacophore of **5** in the 3- and 4-position of the pyrrolidine **6**, (2) allow the extended DPP4 binding pocket to be probed with nitrogen substitution and (3) provide a structurally novel series of DPP4 inhibitors. Given the synthetic accessibility of substituted pyrrolidines and the ready availability of protein co-crystal structures of inhibited complexes, this strategy provides an iterative and rapid approach for inhibitor optimization. Here we report the design, development, and pharmacological evaluation of a novel series of pyrrolidine-constrained phenethylamine inhibitors of DPP4.

N-Substituted pyrrolidines were synthesized according to Scheme 1. Nitrostyrene **7** was treated with the azomethine ylide generated from the action of AgF upon *N*-benzyl-*N*-cyanomethyl-*N*-trimethylsilylamine to provide pyrrolidine **8** (±).[15] Reduction of **8** (±) with zinc dust gave inhibitor **9** (±). Intermediate **8** (±) was debenzylated with triphosgene[16] and the resulting carbamoyl chloride was intercepted with secondary amines to provide tetra-substituted urea inhibitors **10a** and **b** (±) after reduction of the nitro group, as before. When palladium-mediated methods were employed to debenzylate the pyrrolidine, competitive hydrogenolysis of the aryl chlorides occurred. Therefore, **8** (±) was debenzylated[17] with β-trimethylsilylethyl chloroformate[18] to give the Teoc-protected pyrrolidine. Nitro reduction, treatment with Boc-anhydride, and Teoc-removal with TASF (tris(dimethylamino)sulfonium difluorotrimethylsilicate) gave key intermediate **12** (±). Acylation of **12** (±) with acetic anhydride, *p*-tosyl chloride, and isocyanates followed by Boc-deprotection with HCl in dioxane gave amide **13** (±), sulfonamide **14** (±), and urea **15a** and **b** (±) inhibitors, respectively. To provide carbamate inhibitors **16a** and **b** (±), alcohols were treated with DSC (*N*,*N*′-disuccinimidyl carbonate) and the mixed carbonates were intercepted in situ with **12** (±)[19] followed by Boc-removal performed as before. Palladium-mediated N-arylation of **12** (±) or nucleophilic aromatic substitution of heteroaryl chlorides under microwave conditions[20] followed by Boc-deprotection was employed to give inhibitors **17** (±) and **18a**–**d** (±). Treatment of **12** (±) with 2,4-dichloropyrimidine gave a mixture of **19a** (±) and **19b** (±), Suzuki cross-coupling reaction of **19a**–**c** (±) with 3-thiophene boronic acid and removal of the Boc-protecting group provided final compounds **20a**–**c** (±).

Azomethine ylide cyclo-addition chemistry employing nitrostyrenes **21a**–**c**, as before, gave **22a**–**c** (±) (Scheme 2). Nitro reduction and amine protection with

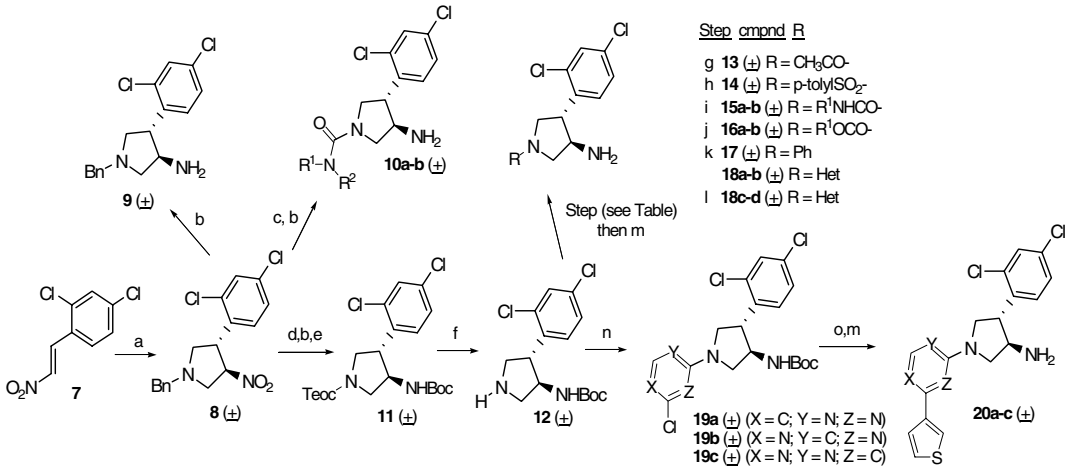

Scheme 1. Reagents and conditions: (a) *N*-benzyl-*N*-cyanomethyl-*N*-trimethylsilylamine, AgF, CH_3CN; (b) Zn, HCl or HOAc, MeOH; (c) triphosgene, CH_2Cl_2 then R^1R^2NH, Et_3N; (d) (c) $ClCO_2CH_2CH_2SiMe_3$, THF; (e) Boc_2O, *i*-Pr_2EtN, THF; (f) TASF, DMF; (g) Ac_2O, *i*-Pr_2EtN, THF; (h) *p*-tosyl chloride, *i*-Pr_2EtN, THF; (i) R^1NCO, *i*-Pr_2EtN, THF; (j) R^1OH, DSC, Et_3N, CH_3CN then **12** (±); (k) RX, Binap, $Pd_2(dba)_3$–$CHCl_3$, *t*-BuONa toluene, 100 °C; (l) RX, *i*-Pr_2EtN, *i*-PrOH, 130 °C, 10 min (microwave); (m) HCl in dioxane; (n) dichloroheterocycle, *i*-Pr_2EtN, *i*-PrOH, 130 °C, 10 min (microwave); (o) 3-thiophene boronic acid, $PdCl_2(PPh_3)_2$, Na_2CO_3, DMF/DME/MeOH/H_2O (1:1:0.9:0.3), 150 °C, 20 min (microwave).

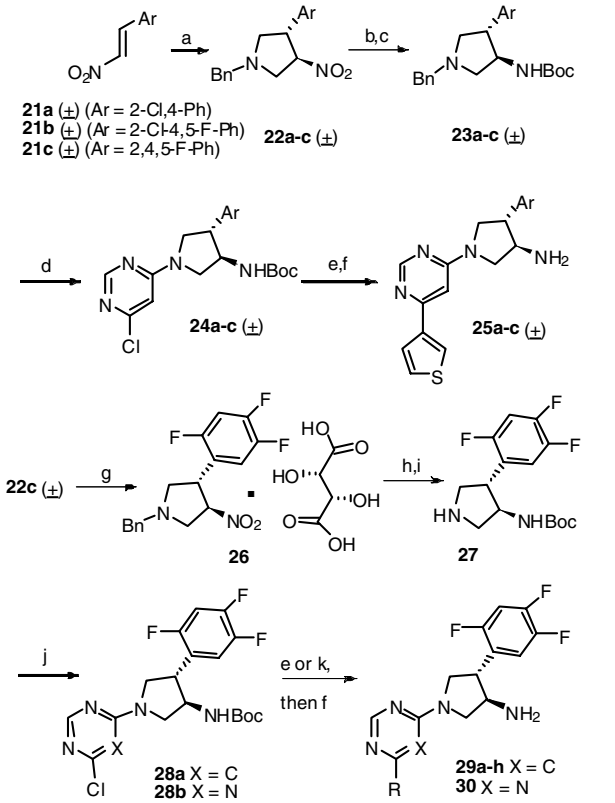

Scheme 2. Reagents and conditions: (a) *N*-benzyl-*N*-cyanomethyl-*N*-trimethylsilylamine, AgF, CH_3CN; (b) Zn, HOAc, MeOH; (c) Boc_2O, *i*-Pr_2EtN, THF; (d) 4,6-dichloropyrimidine, DME, 160 °C, 30 min (microwave); (e) boronic acid, $PdCl_2(PPh_3)_2$, Na_2CO_3, DMF/DME/MeOH/H_2O (1:1:0.9:0.3), 150 °C, 20 min (microwave); (f) HCl in dioxane; (g) D-tartaric acid; (h) RaNi, H_2, EtOH, 40 psi then Boc_2O, THF; (i) $Pd(OH)_2$, MeOH, 50 °C, 60 psi; (j) dichloroheterocycle; (k) $Me_3SnSnMe_3$, $Pd(PPh_3)_4$, dioxane, 105 °C, then ArX, $Pd(PPh_3)_4$, dioxane, 135 °C, 1 h (microwave).

Boc-anhydride provided **23a**–**c** (±). Quaternization of the *N*-benzyl pyrrolidine of **23a**–**c** (±) under microwave conditions using 4,6-dichloropyrimidine was accompanied by debenzylation,[21] and gave a convenient and time saving synthesis of **24a**–**c** (±). Suzuki coupling with 3-thiophene boronic acid was employed to provide inhibitors **25a**–**c** (±) after Boc-deprotection, as before. To provide enantiopure material, D-tartaric acid was used to resolve **22c** (±).[22] The salt **26** was free-based and the nitro group was reduced with Raney nickel to give the free amine. Boc-anhydride protection was followed by debenzylation to give **27**. Substitution of 4,6-dichloropyrimidine or 2,4-dichlorotriazine with **27** gave **28a** or **28b**, respectively. Suzuki cross-coupling with aryl or heteroaryl boronic acids was employed to provide inhibitors **29a**–**e**, **g** and **30**, after Boc-removal. Treatment of **28a** with $(Me_3Sn)_2$ provided a suitable intermediate for Stille cross couplings. In situ coupling with aryl bromides and Boc-deprotection gave final compounds **29f**,**h** in a convenient one-pot procedure.

The cyclohexenyl ring of screening hit **5** (±) serves to efficiently constrain the aryl and amine substitutents, directing the aryl group to the hydrophobic S1 binding pocket and positioning the amine to interact with residues Glu205 and Glu 206 (Fig. 1a). Accordingly, substitution of the distal positions of the cyclohexene directs substituents to productive binding regions. It was apparent that by 'lead-hopping' to pyrrolidines **6**, a nitrogen handle would be introduced in a strategic position to probe the binding pocket with a range of nitrogen substituents. In addition, substitution of the pyrrolidine nitrogen, from a synthetic chemistry perspective, may simplify analoging by allowing for the use of parallel chemistry schemes. A number of N-substituted pyrrolidine inhibitors were tested as racemates against DPP4 (Table 1). It was typical that alkyl, acyl, and sulfonyl-substituted pyrrolidines were poor inhibitors of DPP4, and compounds **9** (±), **13** (±), and **14** (±), respectively, (K_i > 2.7 μM) are representative. However, simple urea **15a** (±) (K_i = 280 nM) and carbamate **16a** (±) (K_i = 490 nM) substitutions increased potency. Diverse libraries of carbamates, tri- and tetra-substituted ureas were prepared to explore the possibility of further gains. However, only modest improvements were observed for our best compounds (urea **15b** (±) K_i = 190 nM, carbamate **16b** (±) K_i = 240 nM). N-Substitution with aryl and heteroaryl groups revealed a clear trend (pyrimidinyl-**18b** (±) (K_i = 210 nM) > pyridyl-**18a** (±) (K_i = 790 nM) > Phe-**17** (±) (K_i = 2800 nM)). A co-crystal structure of **18b** with human DPP4 (Fig. 1b) was analogous to that observed for **5** above in positioning the dichlorophenyl group within the S1 pocket and the primary amine between Glu 205 and Glu 206. The *N*-pyrimidinyl group is observed to stack against the phenyl ring of Phe 357. The potency of **18b**, relative to the other analogs, is likely due to some combination of (1) minimal steric clash between the ortho pyrimidine nitrogens with the pyrrolidine ring system, and/or (2) pi-stacking of the electron-deficient pyrimidine system with Phe 357.

In a separate chemical effort, we have previously reported on thiazole-based peptidomimetic inhibitors of DPP4 (**31** shown in Fig. 1c inset).[23] In this early work, we were able to obtain a number of crystal structures of inhibited rat DPP4 enzyme. The binding mode shown in Figure 1c is representative. Overlay of this structure with the structure of **18b** is shown in Figure 1c and provided a key insight in further analoging of **18b**. While **31** and **18b** bind in a very different manner in the S1 pocket, the two structures converge with the amide of **31** stacking against Phe357 and projecting its thiazole substituent toward Arg358. The excellent overlay of the two structures strongly suggested that gains in potency may be realized by extending heterocyclic, or properly functionalized, aromatic substituents from the meta-position of the pyrimidine of **18b**. An early indication of direction dependence was observed in the relative potencies of meta-substituted **18d** (±) (K_i = 140 nM) and para-substituted **18c** (±) (K_i = 430 nM). A substantial gain in potency was observed for thiophene-substituted compounds with concomitant optimization of the positions of the pyrimidine nitrogens, as evidenced by compound **20c** (±) (K_i = 15 nM) that represents a >50-fold improvement over the initial screening lead.[24] The co-crystal structure of **20c** confirms our design hypothesis (Fig. 1d) with the thiophene projecting into a mainly

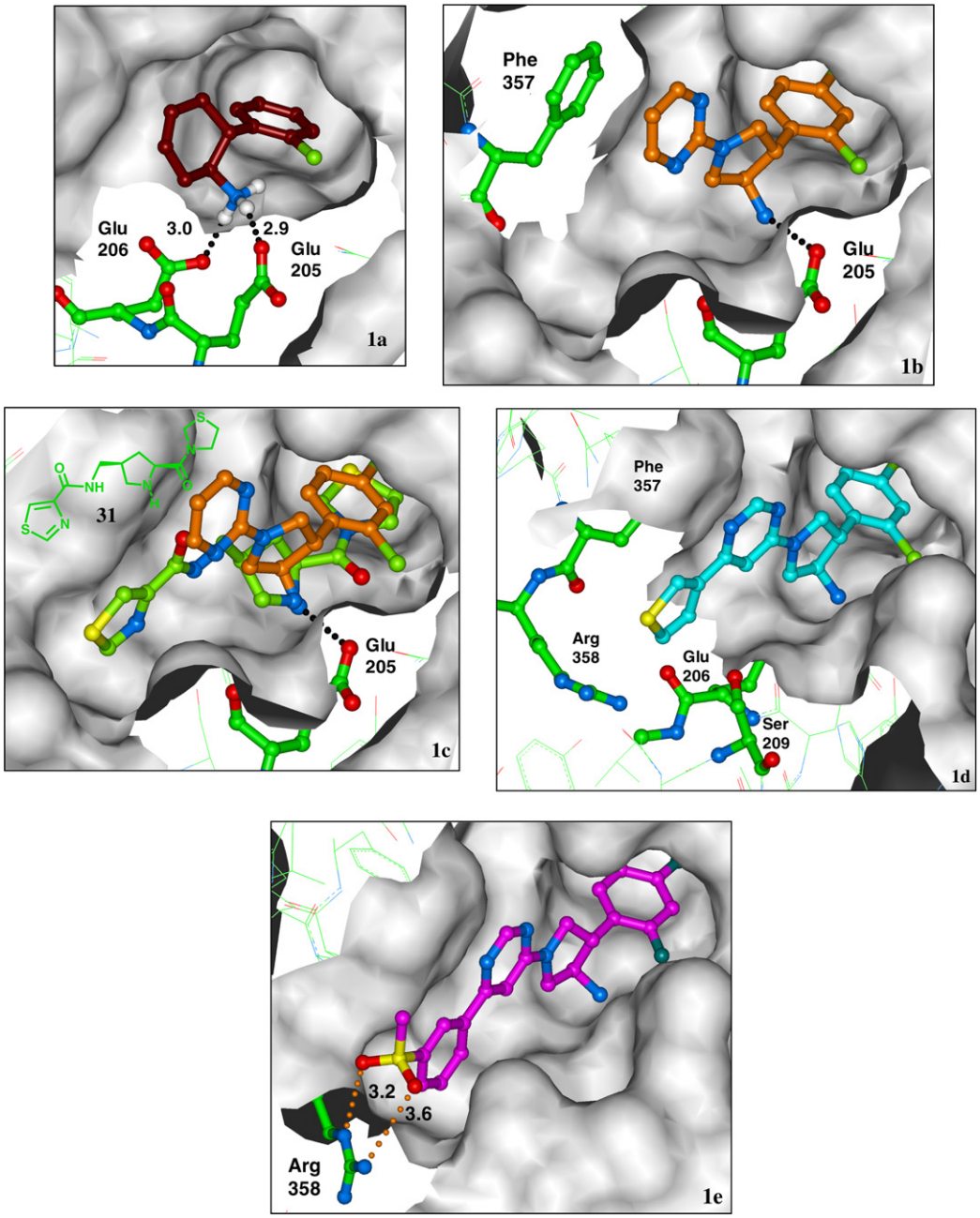

Figure 1. DPP4 co-crystal structures with inhibitors. The source of the DPP4 (human or rat) is indicated. (1a) Compound **5** (brown) in active site of rat DPP4 outlined with gray protein surface. The 2-chlorophenyl group projects into hydrophobic S1 pocket. Hydrogen bonds (N–O distances in Å) are shown as black dotted line between primary ammonium group of **5** and Glu 203-Glu 204 of rat DPP4 (Glu 205–206 of human DPP4). (1b) Compound **18b** (orange) in human DPP4. Glu 205 and Phe 357 (green) are exposed to show polar and pi-stacking interactions, respectively. (1c) Same as Figure 1a with the rat structure of compound **31** (green, pdb code 2OAE) overlaid. The chemical structure of **31** is shown in upper left as an inset. (1d) Compound **20c** (light blue) in human DPP4 with surface removed to expose environment surrounding thiophene ring: Phe 357 C and CB, Arg 358 CB, CG, and CD, Glu 206 O, and Ser 209 OG. (1e) Compound **29g** (pink, pdb code 2OAG) in human DPP4 with polar interactions with Arg 358 guanidinium group highlighted with orange dotted lines.

hydrophobic pocket comprised of Phe 357 C and CB, Arg 358 CB, CG, and CD, Glu 206 O, and Ser 209 OG. The S1-pocket was probed with various halogen substitution patterns (**20c** (±), **25a**–**c** (±)) showing 2,4-dichloro- and 2,4,5-trifluorosubstitution (**25c**, K_i = 17 nM) to be equipotent. Further work in this series used the 2,4,5-trifluoro-pattern to impart compounds with lower C$\log P$, lower molecular weights, and improved chemical orthogonality for further analoging.[25]

From this point on, all 2,4,5-trifluoro analogs were prepared as single enantiomers. In accord with the protein crystal structure, compound **29b** (as drawn in Scheme 2, K_i = 6 nM, Table 2) was the active enantiomer of **25c** (±).[26]

At this point in the research program, a modified enzyme assay was required to assess highly potent compounds with low-nanomolar inhibitory potency.

Table 1. DPP4 inhibition constants of **9**–**18b**[a]

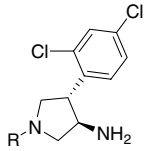

Compound	R	K_i (nM)
9 (±)	Bn–	3400
13 (±)	MeCO–	2700
14 (±)	*p*-TolylSO_2–	13,000
15a (±)	EtNHCO–	280
15b (±)	(3-F)PhCH_2NHCO–	190
10a (±)	EtNMeCO–	610
10b (±)	(3-MeO)PhCH_2NMeCO–	220
16a (±)	EtOCO–	490
16b (±)	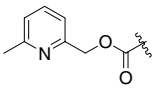	240
17 (±)	Ph–	2800
18a (±)		790
18b (±)		210

[a] All K_i values are an average of at least two runs.

Table 2. DPP4 inhibition constants of **18c**–**25c**[a]

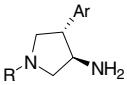

Compound	R	Ar	K_i (nM)
18c (±)	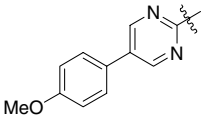	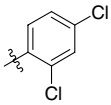	430
18d (±)	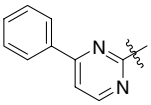	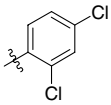	140
20a (±)	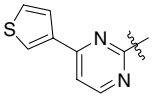	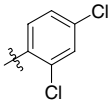	76
20b (±)	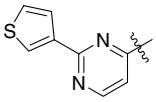	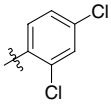	200
20c (±)	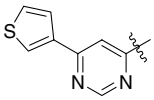	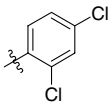	15
25a (±)	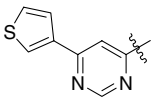	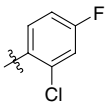	34
25b (±)	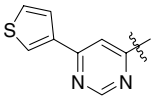	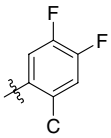	35
25c (±)	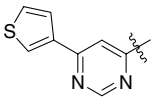	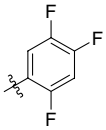	17

[a] All K_i values are an average of at least two runs.

Therefore, a second 'tight binding' assay was utilized (Table 3, K_i (TB)). In addition, a third DPP4 assay in rodent plasma was added to gauge the effect of compound potency in the presence of plasma proteins (K_i TB; 10% PL (rat plasma)). Realizing the close proximity of cationic side chain of Arg 358 to the terminal aryl of compounds like **18d** or **20c**, anionic analogs were prepared to exploit potential electrostatic interactions. Substitution of the pyrimidine with a 3-carboxyphenyl group provided one of the most potent compounds in our series (**29c**, K_i = 1.8 nM (TB)) and represents a 10× improvement over aryl substitution alone (**29a**, K_i = 20 nM). In addition, **29c** was unaffected by plasma protein binding (K_i = 1.0 nM (TB, 10% PL)). Potency gains for similarly positioned polar groups formed a solid trend with small amides (**29e**, K_i = 7 nM), sulfonamides (**29f**, K_i = 3.2 nM (TB), K_i = 1.7 nM (TB, 10%PL)), and sulfones (**29g**, K_i = 3.4 nM (TB), K_i = 3.5 nM (TB, 10%PL)) possessing good potencies and low protein binding. Substitution of the pyrimidine with a 4-carboxyphenyl group did not result in the same gains (**29d**, K_i = 85 nM), and the potency of compounds such as **29g**, when substituted with additional small groups on the aromatic ring (5-fluoro,**29h**, K_i = 9 nM), was compromised. Additional increases in potency were observed when the pyrimidinyl ring of **29g** was replaced with a triazinyl ring (**30**, K_i = 2.1 nM (TB)). The 2-fold gain in potency of the triazinyl ring over the pyrimidine ring may be due to increased pi-stacking interaction with Phe 357 of the enzyme, although differential solvation of the two ring systems or subtle differences in bond angles or bond lengths can not be eliminated from consideration. The crystal structure of **29g** in DPP4 is shown in Figure 1e and exhibits the same binding site interactions identified above with the notable addition of specific H-bonding with the guanidine of Arg 358. Both of the sulfonyl oxygens can be positioned within H-bond distance of Arg 358 (3.2 and 3.6 Ang) in a chelation-arrangement, although we cannot eliminate mono-dentate interpretations from consideration. The most potent compounds of our series that are substituted in the meta-position exploit this interaction and represent a >400x improvement over the initial screening hit.

Compounds **29c**,**f**,**g** and **30** were evaluated (Table 4) in vitro against the human DPP4 homologs DPP8,[27] DPP9,[28] prolyl oligopeptidases (POP),[29] and fibroblast activation protein α (FAPα, also called seprase).[30] While there are a number of other dipeptidyl peptidases in the

Table 3. DPP4 inhibition constants of **29a**–**30**[a]

Compound	R	K_i (nM)	K_i (10%PL, nM)
29a	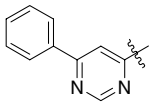	20	nd[c]
29b	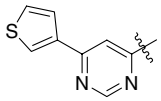	6	nd
29c	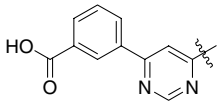	1.8[b]	1.0
29d	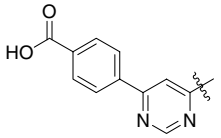	85	nd
29e	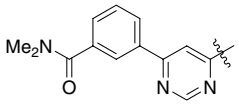	7	nd
29f	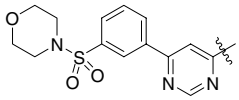	3.2[b]	1.7
29g	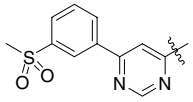	3.4[b]	3.5
29h	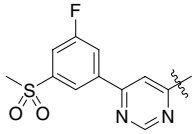	9	nd
30	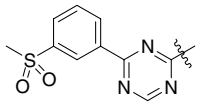	2.1[b]	1.3

[a] All K_i values are an average of at least two runs.
[b] Tight-binding assay (see text).
[c] nd, not determined.

body, the function of most of these peptidases remains unknown at present. There is, however, evidence indicating that DPP8/9 activity may lead to profound toxicity in preclinical species.[31] No inhibition of POP and FAP was observed when compounds were tested at concentrations up to 30 μM. Inhibitors tested against DPP8 and DPP9 had little activity (K_i = 4–6 μM and K_i = 10.9–17 μM, respectively) and, therefore, high levels of selectivity for DPP4.

Early assessment of the ADME characteristics of compounds in the pyrrolidine series indicated that protein binding was low since all compounds measured were <95% protein bound (100% human plasma) and K_i value shifts were not seen for binding studies in the presence of 10% rat plasma (Table 3). In addition, all compounds tested displayed acceptable stabilities in rat and human liver microsome incubation studies ($t_{1/2}$ > 3 h). However, inhibition of CYP2D6 was observed for several racemic compounds (Table 5) including **25c** (±) (IC_{50} = 0.098 μM). Fortuitously, the enantiomer with activity toward DPPIV, **29b**, was >10× less potent toward CYP2D6 (IC_{50} = 1.1 μM). In addition, inhibitors with arene substituents that provided some of our most potent compounds against DPP4 (**29c**,**f** and **30**) lacked CYP2D6 inhibition altogether (IC_{50} = >10 μM).

The pharmacokinetics of several compounds were evaluated in Sprague–Dawley rats (Table 6). Both carboxylic acid-substituted **29c** and sulfonamide-substituted **29f** possessed relatively high clearance rates (CLp 1.10 L/h kg and 2.09 L/h kg, respectively) and low AUCs (po 652 ng h/kg and 515 ng h/kg, respectively). Clearance rates for amide-substituted **29e** were lower and lead to a higher AUC and moderate bioavailability (% F = 42). Sulfones **29g** (% F = 110) and **30** (% F = 74) had excellent bioavailability characterized by high AUCs in rat. Compound **30** was tested in two additional species. In cynomolgus monkey, clearance was higher than in rat (CLp 0.62 L/h kg vs 0.21 L/h kg, respectively) and somewhat lower bioavailability was observed (% F = 42). The bioavailability of **30** in beagle dog was high (% F = 100) and was characterized by high AUC and an extended half-life ($t_{1/2}$ (po, h) = 14.9).

Compound **30** was chosen for in vivo evaluation due to its excellent in vitro potency, selectivity, and pharmacokinetic profile (Fig. 2). Blood glucose lowering was demonstrated in female Zucker diabetic fatty (ZDF) rats of 10 weeks of age that were orally dosed with **30** (t = −240 min), and after four hours of incubation

Table 4. Selectivity of representative DPP4 inhibitors[a]

Compound	DPP4[b]	DPP8	DPP9	POP	FAPα
29c	1.8	>3000	>3000	>30,000	>30,000
29f	3.2	4320	17,500	>30,000	>30,000
29g	3.4	6440	10,900	>30,000	>30,000
30	2.1	4350	11,100	>30,000	>30,000

[a] K_i values (nM) for each enzyme are reported.
[b] K_i values for DPP4 are from tight-binding assay. For structures of the compounds, see Table 3.

Table 5. CYP Inhibition[a]

Compound	CYP2D6 (μM)	CYP2C9 (μM)	CYP3A4 (μM)
25c (±)	0.098	>10	>10
29b	1.1	>10	>10
29c	>10	>10	>10
29f	>10	>10	>10
30	>10	>10	>10

[a] All IC_{50} values are an average of at least two runs. For structures, see Tables 2 and 3.

Table 6. PK profile of selected DPP4 inhibitors

Compound	Species	CLp (L/h kg)	V_{ss} (L/kg)	C_{max} (ng/mL)	$t_{1/2}$ (po, h)	AUC (po) (ng h/kg)	F (%)
29c	Rat	1.10	1.78	176	6.8	652	18
29e	Rat	0.73	1.77	1270	3.5	3144	42
29f	Rat	2.09	1.84	347	1.1	515	21
29g	Rat	0.26	1.44	1813	3.8	22,026	110
30	Rat	0.15	1.15	1970	5.5	24,400	74
30	Monkey	0.62	3.83	218	6.2	1719	42
30	Dog	0.21	4.01	691	14.9	12,203	100

CLp, plasma clearance; V_{ss}, volume of distribution at steady state; C_{max}, maximal concentration when dosed orally; $t_{1/2}$, terminal half-life when dosed orally; AUC, area under curve, F, oral bioavailability.
PK was measured in rats at 5 mg/kg dose. PK was measured in dog and monkey at 2.5 mg/kg dose. For structures, see Table 3.

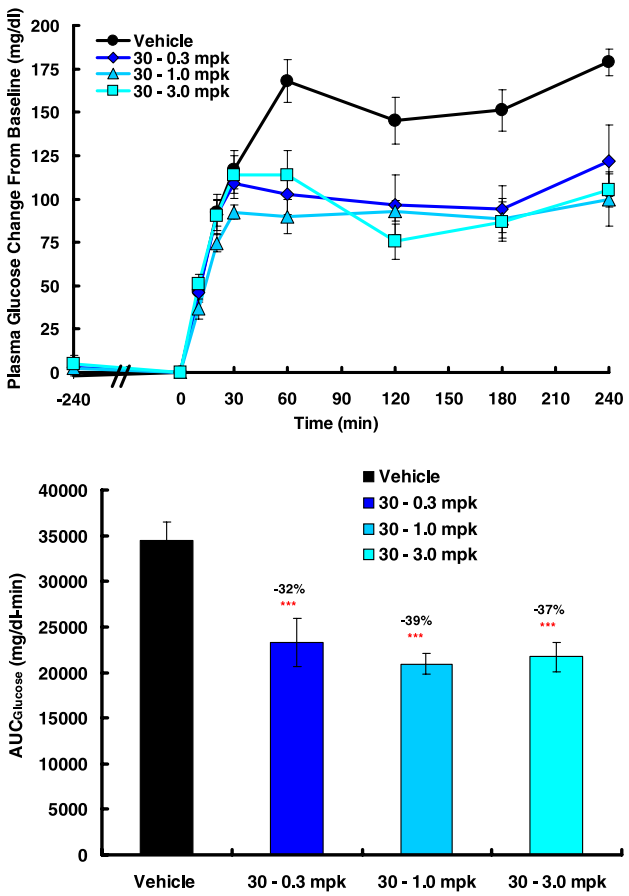

Figure 2. A free-feeding model of female ZDF rats dosed with **30** orally. Overnight fasted female ZDF rats (n = 10/group) of 10 weeks of age were dosed with either vehicle or DPP4 inhibitor **30**. After four hours of pre-incubation with **30**, the rats were allowed to feed (t = 0) freely on a highly palatable, macronutrient balanced food source (64% CHO, 22% fat, and 14% Pro) and during which blood glucose levels were measured. Plasma glucose change from baseline is shown on the left panel and area under the curve (AUC) change (t = 0 to t = 240 min) is shown on the right panel.

with **30**, were allowed to feed freely on a balanced food source (t = 0 min). This model is analogous to oral glucose tolerance tests (OGTT) used clinically to evaluate glycemic control, except that the 'challenge' is a liquid mixed meal composed of fats, proteins, and carbohydrates, and thus a more realistic representation of the nutritional makeup of normal food. Glucose excursion as measured by the area under the curve (AUC) was lowered at all three doses (0.3 mg/kg, −32%; 1 mg/kg, −39%; 3 mg/kg −37%) in comparison to the vehicle. The plasma concentration of **30** reached 686 ± 48 ng/mL (t = 0) and 373 ± 45 ng/mL (t = 240), providing >99% (t = 0) and >98% (t = 240 min) inhibition of DPP4 at 1 mpk, respectively.

In conclusion, a 'lead-like' screening hit inspired the development of a series of pyrrolidine-constrained DPP4 inhibitors. By lead-hopping to the synthetically flexible pyrrolidine framework and employing structure-based design, significant gains in potency (>400×) were realized in rapid fashion. ADME characteristics, in vitro potency, and selectivity characteristics were optimized in parallel to provide several compounds with attractive profiles. Optimized compounds were very potent DPP4 inhibitors with a low degree of protein binding and high selectivity against DPP4 homologs. Compound **30** possessed attractive pharmacokinetic profiles in multiple preclinical species. In addition, **30** was quite efficacious in vivo, lowering the blood glucose of rats when orally dosed prior to a mixed meal.

Supplementary data

X-ray crystal structures have been deposited in the RCSB protein data bank (www.rcsb.org) with codes 2OAE and 2OAG. Supplementary data associated with this article can be found, in the online version, at doi:10.1016/j.bmcl.2007.01.026.

References and notes

1. Zander, M.; Madsbad, S.; Madsen, J. L.; Holst, J. J. *Lancet* **2002**, *359*, 824.
2. (a). *Diabetologia* **1992**, *35*, 701; For reviews see: (b) Holst, J. J. *Gastroenterology* **1994**, *107*, 1048; (c) Drucker, D. J. *Diabetes* **1998**, *47*, 159; (c) Deacon, C. F.; Holst, J. J.; Carr, R. D. *Drugs Today* **1999**, *35*, 159.
3. (a) Wettergren, A.; Schjoldager, B.; Mortensen, P. E.; Myhre, J.; Christiansen, J.; Holst, J. J. *Dig. Dis. Sci.* **1993**, *38*, 665; (b) Nauck, M. A.; Niedereichholz, U.; Ettler, R.; Holst, J. J.; Orskov, C.; Ritzel, R.; Schmiegel, W. H. *Am. J. Physiol.* **1997**, *273*, E981.
4. Flint, A.; Raben, A.; Ersboll, A. K.; Holst, J. J.; Astrup, A. *Int. J. Obes.* **2001**, *25*, 781.
5. Farilla, L.; Hui, H.; Bertolotto, C.; Kang, E.; Bulotta, A.; Di Mario, U.; Perfetti, R. *Endocrinology* **2002**, *143*, 4397.

6. (a) Kieffer, T. J.; McIntosh, C. H. S.; Pederson, T. A. *Endocrinology* **1995**, *136*, 3585; (b) Deacon, C. F.; Nauck, M. A.; Toft-Nielson, M.; Pridal, L.; Willms, B.; Holst, J. J. *Diabetes* **1995**, *44*, 1126.
7. (a) Ahrén, B.; Simonsson, E.; Larsson, H.; Landin-Olsson, M.; Torgeirsson, H.; Jansson, P.-A.; Sandqvist, M.; Bavenholm, P.; Efendic, S.; Eriksson, J. W.; Dickinson, S.; Holmes, D. *Diabetes Care* **2002**, *25*, 869; (b) Ahrén, B.; Gomis, R.; Standl, E.; Mills, D.; Schweizer, A. *Diabetes Care* **2004**, *27*, 2874; (c) Ahrén, B.; Landing-Olsson, L.; Jansson, P-A.; Sevensson, M.; Holmes, D.; Schweizer, A. *J Clin. Endocrinol. Metab.* **2004**, *89*, 2078; (d) Ahrén, B.; Pacini, G.; Foley, J. E.; Schweizer, A. *Diabetes Care* **2005**, *28*, 1936.
8. Villhauer, E. B.; Brinkman, J. A.; Naderi, G. B.; Burkey, B. F.; Dunning, B. E.; Prasad, K.; Mangold, B. L.; Russell, M. E.; Hughes, T. E. *J. Med. Chem.* **2003**, *46*, 2774.
9. Kim, D.; Wang, L.; Beconi, M.; Eiermann, G. J.; Fisher, M. H.; He, H.; Hickey, G. J.; Kowalchick, J. E.; Leiting, B.; Lyons, K.; Marsilio, F.; McCann, M. E.; Patel, R. A.; Petrov, A.; Scapin, G.; Patel, S. B.; Sinha Roy, R.; Wu, J. K.; Wyvratt, M. J.; Zhang, B. B.; Zhu, L.; Thornberry, N. A.; Weber, A. E. *J. Med. Chem.* **2005**, *48*, 141.
10. Augeri, D. J.; Robl, J. A.; Betebenner, D. A.; Magnin, D. R.; Khanna, A.; Robertson, J. G.; Wang, A.; Simpkins, L. M.; Taunk, P.; Huang, Q.; Han, S-P.; Abboa-Offei, B.; Cap, M.; Xin, L.; Tao, L.; Tozzo, E.; Welzel, G. E.; Egan, D. M.; Marcinkeviciene, J.; Chang, S. Y.; Biller, S. A.; Kirby, M. S.; Parker, R. A.; Hamann, L. G. *J. Med. Chem.* **2005**, *48*, 5025.
11. Madar, D. J.; Kopecka, H.; Pireh, D.; Yong, H.; Pei, Z.; Li, X.; Wiedeman, P. E.; Djuric, S. W.; Von Geldern, T. W.; Fickes, M. G.; Bhagavatula, L.; McDermott, T.; Wittenberger, S.; Richards, S. J.; Longenecker, K. L.; Stewart, K. D.; Lubben, T. H.; Ballaron, S. J.; Stashko, M. A.; Long, M. A.; Wells, H.; Zinker, B. A.; Mika, A. K.; Beno, D. W. A.; Kempf-Grote, A. J.; Polakowski, J.; Segreti, J.; Reinhart, G. A.; Fryer, R. M.; Sham, H. L.; Trevillyan, J. M. *J. Med. Chem.* **2006**, *49*, 6416.
12. Oprea, T. I.; Davis, A. M.; Teague, S. J.; Leeson, P. D. *J. Chem. Inf. Comput. Sci.* **2001**, *41*, 1308.
13. Abad-Zapatero, C.; Metz, J. T. *Drug Discovery Today* **2005**, *10*, 464.
14. Lead-like hit **5** has been optimized to provide a clinical candidate Pei, Z.; Li, X.; von Geldern, T. W.; Madar, D. J.; Longenecker, K.; Yong, H.; Lubben, T. H.; Stewart, K. D.; Zinker, B. A.; Backes, B. J.; Judd, A. S.; Mulhern, M.; Ballaron, S. J.; Stashko, M. A.; Mika, A. K.; Beno, D. W. A.; Reinhart, G. A.; Fryer, R. M.; Preusser, L. C.; Kempf-Grote, A. J.; Sham, H. L.; Trevillyan, J. M. *J. Med. Chem.* **2006**, *49*, 6439.
15. Padwa, A.; Chen, Y. Y. *Tetrahedron Lett.* **1984**, *25*, 5739.
16. Jorand-Lebrun, C.; Valognes, D. *Synth. Commun.* **1998**, *23*, 1189.
17. Cambell, A. L.; Pilipauskas, D. R.; Khanna, I. K.; Rhodes, R. A. *Tetrahedron Lett.* **1987**, *28*, 2331.
18. Shute, R. E.; Rich, D. H. *Synthesis* **1987**, 346.
19. Hamilton, G. L.; Backes, B. J. *Tetrahedron Lett.* **2006**, *47*, 967.
20. Luo, G.; Chen, L.; Poindexter, G. S. *Tetrahedron Lett.* **2002**, *43*, 5739.
21. Hamilton, G. L.; Backes, B. J. *Tetrahedron Lett.* **2006**, *47*, 2229.
22. A matrix of chiral acids (D-tartaric acid, D-malic acid, (1*R*)-(−)10-camphorsulfonic acid, and (*R*)-(−)-mandelic acid) and solvents (THF, EtOH, EtOAc and acetone) were evaluated to resolve **21c** (±). The use of D-tartaric acid and EtOH provided a practical solution.
23. Shuai, Q.; Patel, J.; Zanze, I.; Dinges, J.; Wiedeman, P.; Pei, Z.; Michmerhuizen, M. J.; Hoff, E.; Kalvin, D. M.; von Geldern, T.; Lubben, T.; Ballaron, S.; Stashko, M.; Zinker, B.; Djuric, S.; Beno, D.; Kempf-Grote, A. J.; Mika, A.; Farb, T.; Perham, M. A.; Adler, A. L.; Trevillyan, J.; Sham H. Acyl thiazolidides-novel potent DPP-IV inhibitors, MEDI Poster 303, *American Chemical Society National Meeting*, Aug 28–Sep 1, 2005; Washington, DC, USA.
24. For initial studies, thiophene substitution was evaluated rather than thiazole substitution since the requisite starting material (thiophene boronic acid) is commercially available.
25. It is noteworthy that **2** (MK-0431) has an aryl group with a similar 2,4,5-trifluorosubstitution pattern as **25c**. We obtained internal co-crystal structures using compounds similar to **2** (Edmondson, D. D.; Parmee, E.; Weber, A. E.; Xu, J. Dipeptidyl Peptidase Inhibitors for the Treatment of Diabetes, Patent WO 03/000180, January 3, 2003). The data indicated that our pyrrolidine-based inhibitors and the Merck inhibitors share a similar aryl binding mode. On that basis, compounds featuring the 2,4,5-trifluorosubstitution pattern were included in our SAR studies.
26. An X-ray crystal structure was obtained from D-tartaric acid salt **26**. The stereochemical assignments of the pyrrolidine substituents of **26** were in agreement with protein crystal structure (Fig. 1d). These data further confirm the stereochemical assignment of **29b** as the active enantiomer of **25c** (±).
27. Abbott, C. A.; Yu, D. M. T.; Woollatt, E.; Sutherland, G. R.; McCaughan, G. W.; Gorrell, M. D. *Eur. J. Biochem.* **2000**, *267*, 6140.
28. Ajami, K.; Abbott, C. A.; McCaughan, G. W.; Gorrell, M. D. *Biochem. Biophys. Acta* **2004**, *1679*, 18.
29. Rosenblum, J. S.; Kozarich, J. W. *Curr. Opin. Chem. Biol.* **2003**, *7*, 496.
30. Scanlan, M. J.; Raj, B. K. M.; Calvo, B.; Garin-Chesa, P.; Sanz-Moncasi, M. P.; Healey, J. H.; Old, L. J.; Rettig, W. J. *Proc. Natl. Acad. Sci. U.S.A.* **1994**, *91*, 5657.
31. Lankas, G. R.; Leiting, B.; Roy, R. S.; Eiermann, G. J.; Beconi, M. G.; Biftu, T.; Chan, C.-C.; Edmondson, S.; Feeney, W. P.; He, H.; Ippolito, D. E.; Kim, D.; Lyons, K. A.; Ok, H. O.; Patel, R. A.; Petrov, A. N.; Pryor, K. A.; Qian, X.; Reigle, L.; Woods, A.; Wu, J. K.; Zaller, D.; Zhang, Z.; Zhu, L.; Weber, A. E.; Thornberry, N. A. *Diabetes* **2005**, *54*, 2988.